Composites Communications 26 (2021) 100776

Contents lists available at ScienceDirect

Composites Communications

journal homepage: www.elsevier.com/locate/coco

Insight into ultra-refined grains of aluminum matrix composites via deformation-driven metallurgy

Yuming Xie [a,1], Xiangchen Meng [a,1], Yulong Li [b], Dongxin Mao [a], Long Wan [a], Yongxian Huang [a,*]

[a] State Key Laboratory of Advanced Welding and Joining, Harbin Institute of Technology, 150001, Harbin, China
[b] Beijing Institute of Space Launch Technology, Beijing, 100076, China

ARTICLE INFO

Keywords:
Severe plastic deformation
Graphene
Aluminum matrix composites
Dynamic recrystallization

ABSTRACT

Ultra-refined grains were obtained in few-layer graphene nanoplatelets reinforced aluminum matrix composites via deformation-driven metallurgy under coupled thermo-mechanical effect. Fragmentation, thinning and re-dispersion of the reinforcements accelerated the nucleation of recrystallized grains and inhibited the migration of grain boundaries. The synergy grain refinement mechanism led to a greatly refined microstructure with an average grain size of 267.0 nm, which was much smaller than the grain size of conventional aluminum matrix composites to realize high strengthening-toughening efficiency. This novel preparation route showed the capacity of developing ultra-fine aluminum matrix composites with the exceptional grain refinement towards ultra-lightweight design.

1. Introduction

Aluminum alloys and aluminum matrix composites have attracted great attention for their light weight and excellent load-bearing capacity, which have been widely utilized in astronautic and aeronautic applications [1–4]. To further enhance their specific strength towards ultra-lightweight design, grain refinement engineering is one of the most effective method [5]. Graphene nanoplatelets (GNPs) have been widely utilized for grain refinement due to the fact that these reinforcements could act as nucleation substrates during liquid-state processing or Zener pinning positions during solid-state processing [6]. Nevertheless, graphene is susceptible to agglomeration due to the great van der Waals force, leading to the unsatisfactory microstructures [7,8]. One of the major issues to ameliorate the refining effect is to conduct efficient redistribution and realize dispersion uniformity of these carbonaceous nanoparticles.

Severe plastic deformation techniques, including friction stir processing, high pressure torsion and equal channel angular pressing, etc., are ideal approaches towards the uniform distribution of reinforcements, as well as the great grain refinement [9,10]. High-value plastic strain performed by external deformation contributes to dynamic recovery/recrystallization of the matrix and fragmentation/dispersion of the nanoparticles, thereby obtaining excellent mechanical performances of aluminum matrix composites [11]. A novel severe plastic deformation technique, deformation-driven metallurgy (DDM) was also proposed by our research group [12,13] to obtain the one-step preparation of the bulk materials from composite powders, which can apply great grain refinement and reinforcement dispersion via high-value strain rate and deformation-driven heat generation. In this paper, DDM was utilized to introduce the ultra-fine microstructures into the aluminum matrix composites reinforced by few-layer GNPs. The solid-state preparation based on blended metallic powders with GNPs further enhances the grain refinement. The synergy mechanism for grain refinement was discussed via severe plastic deformation and evolution behavior of the reinforcements.

2. Material and methods

Few-layer GNPs and pure aluminum powders with average diameter of respectively 1–3 μm and 10 μm were chosen as raw powders. The addition of GNPs in the composites was 1.5 wt%. Ball milling in argon atmosphere was conducted to obtain the fully-blended powders with the milling time of 10 h and rotational velocity of 200 rpm. The milled powders were then sifted out and placed in an aluminum mould. A processing tool rotating at the rotational velocity of 1000 rpm pressed the material up to 180 s. Then densified aluminum matrix composites

* Corresponding author.
E-mail address: yxhuang@hit.edu.cn (Y. Huang).
[1] These authors contributed equally to this work.

https://doi.org/10.1016/j.coco.2021.100776
Received 23 February 2021; Received in revised form 1 April 2021; Accepted 27 April 2021
Available online 12 May 2021

were obtained by frictional heat input and severe plastic deformation. The final diameter of the composites disc was 16 mm and the thickness was 1.0 mm. The detailed DDM procedure, were illustrated in Fig. 1a. More details can be found in our previous work [12,13].

Following the DDM process, tensile specimens with a gauge length of 5 mm and width of 1.4 mm were machined and tested were conducted at a strain rate of $1 \times 10^{-3}\ s^{-1}$ at room temperature. Three specimens were tested for each parameter. The samples were characterized by Raman spectroscopy and X-ray photoelectron spectroscopy (XPS) to obtain the chemical evolution. The microstructures including grain sizes and dispersion of GNPs were observed by electron backscatter diffraction (EBSD) and transmission electron microscopy (TEM), respectively.

3. Results and discussion

Fig. 1a illustrates the detailed DDM procedure and Fig. 1b shows the macroscopic formation of the composites. The composite discs have a diameter of 16 mm and a thickness of 1 mm. Sound composites are obtained and continuous streamline with the shape of Archimedes spiral is observed on the upper surface, implying that the composites experienced sliding friction and severe plastic deformation induced by DDM. The ultimate tensile strength and elongation reached 468 ± 7 MPa and 19.9 ± 0.6% at the processing time of 60 s, showing a strengthening efficiency of 293.3% with almost no ductility loss compared to the pure aluminum prepared by DDM (Fig. 1c). A finite element analysis was conducted to quantify the coupled thermo-mechanical effect and microstructural evolution, as shown in Fig. 1d. Since the temperature basically reaches the quasi-steady state after 60 s, the maximum time axis of Fig. 1d is 120 s. The contours of quasi-steady temperature and equivalent plastic strain at 60 s show that each micro zone of the disc experienced significantly different heat input and plastic deformation. The quasi-steady temperature gradually decreased as the distance from center of the disc increased. The temperature range is about 660–760 K, which are all higher than the minimum temperature required for dynamic recrystallization of aluminum ($0.5T_m \sim 467$ K) [14]. Besides, the whole composites undergo great accumulative plastic deformation. The synthesis combination implies that sufficient dynamic recrystallization occurs to refine the microstructures. In addition, the transient temperature does not reach a constant value at the beginning of the DDM process. The temperature gradually rises during the first 60 s, indicating that there is a stage where the grains are modified by cold deformation without recrystallization.

Raman spectroscopy can characterize the evolution of GNPs (Fig. 2a). The ratio of D-band to G-band shows the fragmentation degree of graphene. The D-band and the G-band represent the breathing mode of A_{1g} symmetry and the stretching mode of sp^2 pairs, respectively [15]. Severe plastic deformation significantly enhances the smashing and dispersion of GNPs. This means that more exposed two-dimensional edges and active sites are produced on the graphene [16], which promotes the chemical bonding between GNPs and aluminum matrix to strengthen the inhibition of GNPs on dislocation rearrangement and grain boundary migration of the matrices during recrystallization and growth. The fragmentation of GNPs gradually increases with the increase of DDM time, indicating that the average diameter of graphene is continuously decreasing. However, excessively broken graphene weakens its load transfer effect, thereby impairing the high strengthening efficiency of GNPs themselves. In addition, the G-band of the DDMed sample has a blueshift compared to the raw powders. This shift of G-band was related to the average number of graphene layers due to the weakening of the bonding energy between graphene layers [17], which can be calculated by the following equation:

$$\omega_G = 1581.6 + \frac{11}{1 + n^{1.6}} \tag{1}$$

where ω_G is the wavenumber of the G-band and n is the number of graphene layers, which was calculated as 5.51, 2.63, 2.45, 2.17 and 1.65 for raw powders, 10 s, 30 s, 60 s and 180 s, respectively. The number of layers decreases with severe plastic deformation, indicating that the DDM process can introduce interlayer slip in GNPs to further improve their dispersion. Similar results can be seen in the deconvoluted C 1s peak of XPS results in Fig. 2b. The gradual increase in the ratio of sp^3 to sp^2 indicates the fragmentation of GNPs. The emergence of C–*O*–Al bond and its gradual substitution by C–Al bond, showing that there is a good chemical bonding between GNPs and matrices [18], thus ensuring the inhibitory effect of graphene on the coarsening of the recrystallized grains. The average grain size of the composite at the preparation time of 60 s is 267.0 nm (Fig. 2c), which is much smaller than the grain size of conventional GNPs reinforced aluminum matrix composites (about several micrometers to tens of micrometers) [19], proving that GNPs are capable of realizing the ultra-refined grains via severe plastic deformation. In addition, the average grain size of the other three preparation time including 10 s, 30 s and 180 s are respectively 214.9 nm, 255.2 nm and 358.8 nm, which will be discussed below.

Fig. 3d depicts the distribution of GNPs in the aluminum matrix composites. The GNPs are uniformly dispersed intergranularly and intragranularly. Those reinforcement located at the grain boundary exhibits obvious pinning effect on the migration of the grain boundary and the inhibitory effect on the rearrangement of dislocations [20]. The

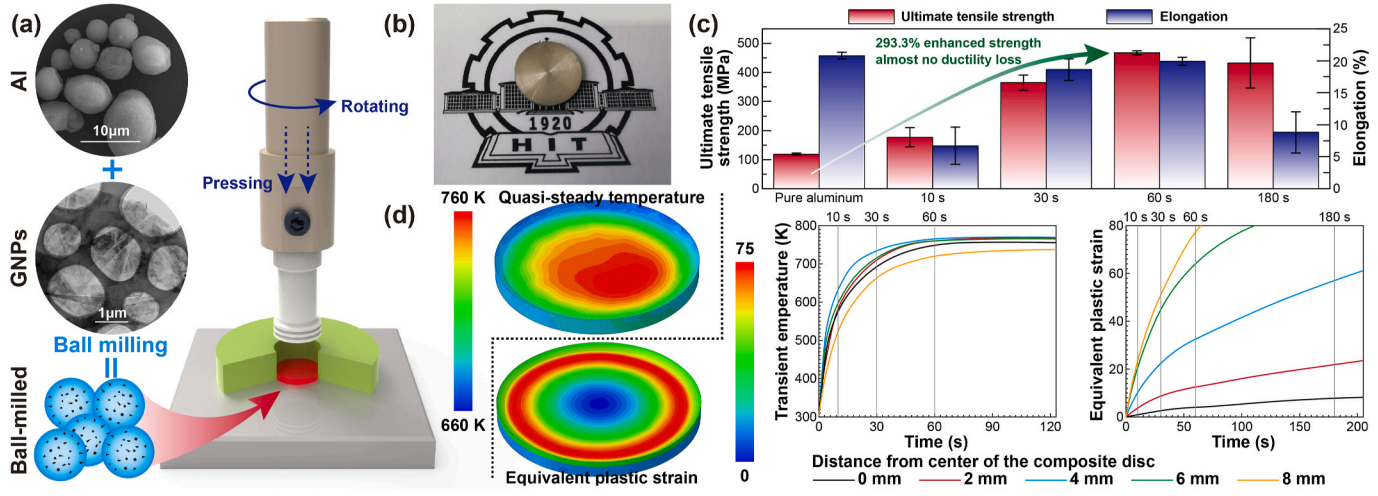

Fig. 1. (a) Schematic of DDM procedure, (b) macrostructures of the typical composite disc, (c) tensile properties of the composites with different processing time and (d) evolution of the temperature and plastic deformation.

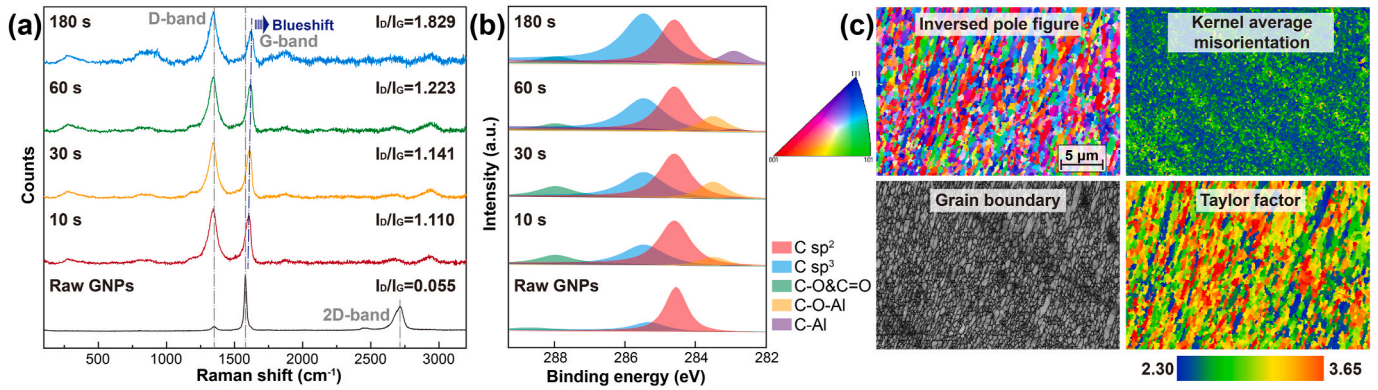

Fig. 2. (a) Raman spectra, (b) XPS results and (c) EBSD images of the DDMed composites.

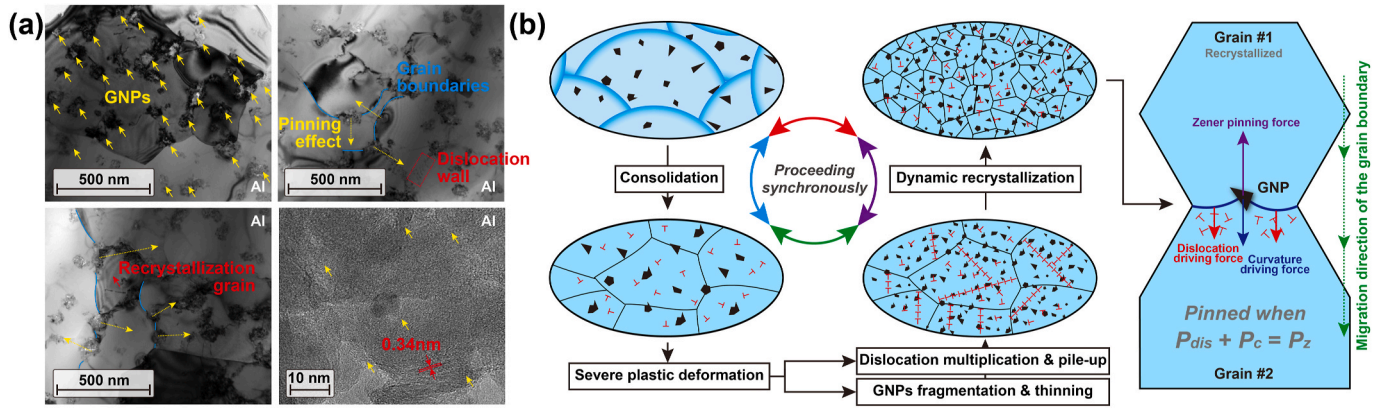

Fig. 3. (a) TEM images of the DDMed composites, and (b) synergy grain refinement mechanism during DDM process.

fragmentation of GNPs and dynamic recrystallization are proven to occur simultaneously during the DDM process. The severe plastic deformation promotes the rapid multiplication of the geometric necessary dislocations and realizes the nucleation of recrystallized grains synchronously. The GNPs suppresses the movement of dislocation, promoting the localized dislocation aggregation and accelerating the dynamic recrystallization [21]. In the subsequent growth process of the recrystallized grains, those GNPs adjacent to the grain boundaries obtain higher defect energy due to the significant fragmentation and re-dispersion behaviors via severe plastic deformation, which further realize the Zener pinning of the grain boundary [22]. This pinning force is inversely proportional to the average size of GNPs [23]. The pinning force produced by the thinned GNPs rapidly balances with the curvature driving force and dislocation driving force, thereby effectively inhibiting the growth of recrystallized grains, and finally obtaining a nano-sized microstructure.

An analytical model was proposed and conducted to grain growth qualitatively, whose detailed information was illustrated in Supplementary Materials. The calculated evolution behaviors of the grain sizes with and without GNPs were obtained as shown in Fig. 4. Nano-sized grain refinement is observed in the composites containing GNPs. The calculated grain diameter with the DDM time of 60 s is 288.9 nm, which is basically in agreement with the experimental results and is reduced by about 82% compared to that of the composites without GNPs. This proves the inhibitory effect of the fragmented and thinned graphene on the migration of recrystallized grain boundaries. Besides, the composites containing GNPs trigger dynamic recrystallization earlier, which is consistent with our previous discussion. The evolution curve includes 5 different stages: Incubation, recrystallization, growth, steady and 2nd growth stages. The first growth stage is attributed to the tiny newly-nucleated grains and insufficient pinning effect. The steady stage

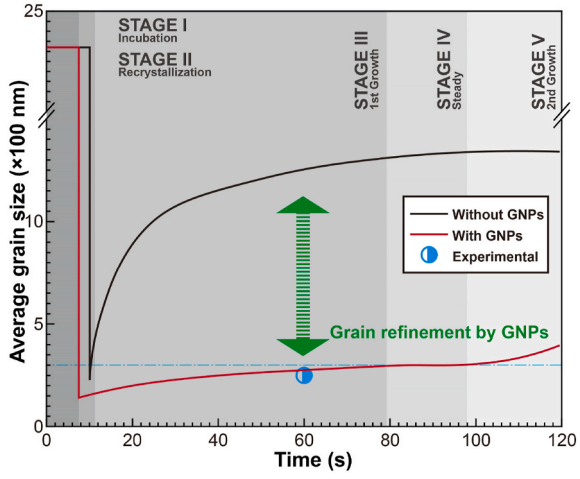

Fig. 4. Evolution behaviors of the grain sizes with and without GNPs.

corresponds to the state where the pinning force and the dislocation/curvature driving force strike a balance. The 2nd growth stage is due to the limitation of fragmentation of the GNPs. It is difficult for GNPs to continue to be thinned and fragmented to provide greater pinning effect, which triggers the migration of the grain boundaries again. The calculated results are consistent with the EBSD results, which proved the accuracy of this model. In addition, the excessive fragmentation of GNPs also damages the Orowan strengthening and load transfer effect, where the detrimental intermetallic compound Al_4C_3 is also susceptible to produce [24]. The better grain refinement needs to be realized by

adjusting the temperature and strain input adequately towards higher strength and ductility.

4. Conclusions

DDM was utilized as a feasible technique for realizing ultra-refined grains of few-layer GNPs reinforced aluminum matrix composites, in which severe plastic deformation and corresponding frictional/deformation heat contributed to solid-state sintering and microstructural modification. Fragmentation, thinning and re-dispersion of GNPs were obtained with the occurrence of dynamic recrystallization. These GNPs suppressed the movement of dislocation, promoting the localized dislocation aggregation and accelerating the dynamic recrystallization in the nucleation stage. They also introduced pinning force to balance with the curvature and dislocation driving force, inhibiting the growth of recrystallized grains effectively to obtain a nano-crystalline microstructure. The average grain size reached 267.0 nm, which was much smaller than the grain size of traditional aluminum matrix composites to realize high strengthening-toughening efficiency, indicating that DDM was capable of enhancing the grain refinement via severe plastic deformation.

CRediT authorship contribution statement

Yuming Xie: Conceptualization, Investigation, Writing – original draft. **Xiangchen Meng:** Methodology, Investigation. **Yulong Li:** Popularization, Application. **Dongxin Mao:** Methodology, Writing – review & editing. **Long Wan:** Methodology, Writing – review & editing. **Yongxian Huang:** Conceptualization, Supervision.

Declaration of competing interest

The authors declare that they have no known competing financial interests or personal relationships that could have appeared to influence the work reported in this paper.

Acknowledgement

This work was jointly supported by the Hei Long Jiang Postdoctoral Foundation (No. LBH-Z20055) and the Youth Program of National Natural Science Foundation of China (No. 52001099).

Appendix A. Supplementary data

Supplementary data to this article can be found online at https://doi.org/10.1016/j.coco.2021.100776.

Data availability

The data that support the findings of this study are available from the corresponding author upon reasonable request.

Code availability

Partial of the code that support the findings of this study are available from the corresponding author. The entire code is not publicly available due to them containing information that could compromise research participant consent.

References

[1] X. Meng, Y. Huang, J. Cao, J. Shen, J.F. dos Santos, Recent progress on control strategies for inherent issues in friction stir welding, Prog. Mater. Sci. 115 (2021) 100706, https://doi.org/10.1016/j.pmatsci.2020.100706.
[2] T. Vogel, S. Ma, Y. Liu, Q. Guo, D. Zhang, Impact of alumina content and morphology on the mechanical properties of bulk nanolaminated Al2O3-Al composites, Compos. Commun. 22 (2020) 100462, https://doi.org/10.1016/j.coco.2020.100462.
[3] K. Venkateswara Reddy, R. Bheekya Naik, G.R. Rao, G. Madhusudhan Reddy, R. Arockia Kumar, Microstructure and damping capacity of AA6061/graphite surface composites produced through friction stir processing, Compos. Commun. 20 (2020) 100352, https://doi.org/10.1016/j.coco.2020.04.018.
[4] D. Dispinar, Bending properties of graphene reinforced aluminium matrix composite produced by casting process, Mod. Concepts Mater. Sci. 3 (2020), https://doi.org/10.33552/MCMS.2020.03.000557.
[5] S.J. Abraham, I. Dinaharan, J.D. Raja Selvam, E.T. Akinlabi, Microstructural characterization of vanadium particles reinforced AA6063 aluminum matrix composites via friction stir processing with improved tensile strength and appreciable ductility, Compos. Commun. 12 (2019) 54–58, https://doi.org/10.1016/j.coco.2018.12.011.
[6] T. Han, J. Li, N. Zhao, C. He, Microstructure and properties of copper coated graphene nanoplates reinforced Al matrix composites developed by low temperature ball milling, Carbon 159 (2020) 311–323, https://doi.org/10.1016/j.carbon.2019.12.029.
[7] P. Shao, G. Chen, B. Ju, W. Yang, Q. Zhang, Z. Wang, X. Tan, Y. Pei, S. Zhong, M. Hussain, G. Wu, Effect of hot extrusion temperature on graphene nanoplatelets reinforced Al6061 composite fabricated by pressure infiltration method, Carbon 162 (2020) 455–464, https://doi.org/10.1016/j.carbon.2020.02.080.
[8] F. Chen, N. Gupta, R.K. Behera, P.K. Rohatgi, Graphene-reinforced aluminum matrix composites: a review of synthesis methods and properties, JOM 70 (2018) 837–845, https://doi.org/10.1007/s11837-018-2810-7.
[9] I. Dinaharan, K. Kalaiselvan, N. Murugan, Influence of rice husk ash particles on microstructure and tensile behavior of AA6061 aluminum matrix composites produced using friction stir processing, Compos. Commun. 3 (2017) 42–46, https://doi.org/10.1016/j.coco.2017.02.001.
[10] J. Li, X. Meng, Y. Li, L. Wan, Y. Huang, Friction stir extrusion for fabricating Mg-RE alloys with high strength and ductility, Mater. Lett. (2021) 129414, https://doi.org/10.1016/j.matlet.2021.129414.
[11] Z.W. Zhang, Z.Y. Liu, B.L. Xiao, D.R. Ni, Z.Y. Ma, High efficiency dispersal and strengthening of graphene reinforced aluminum alloy composites fabricated by powder metallurgy combined with friction stir processing, Carbon 135 (2018) 215–223, https://doi.org/10.1016/j.carbon.2018.04.029.
[12] Y. Xie, X. Meng, Y. Huang, J. Li, J. Cao, Deformation-driven metallurgy of graphene nanoplatelets reinforced aluminum composite for the balance between strength and ductility, Compos. B Eng. 177 (2019) 107413, https://doi.org/10.1016/j.compositesb.2019.107413.
[13] Y. Xie, Y. Huang, F. Wang, X. Meng, J. Li, Z. Dong, J. Cao, Deformation-driven metallurgy of SiC nanoparticle reinforced aluminum matrix nanocomposites, J. Alloys Compd. 823 (2020) 153741, https://doi.org/10.1016/j.jallcom.2020.153741.
[14] T. Sakai, A. Belyakov, R. Kaibyshev, H. Miura, J.J. Jonas, Dynamic and post-dynamic recrystallization under hot, cold and severe plastic deformation conditions, Prog. Mater. Sci. 60 (2014) 130–207, https://doi.org/10.1016/j.pmatsci.2013.09.002.
[15] S. Saadallah, A. Cablé, S. Hamamda, K. Chetehouna, M. Sahli, A. Boubertakh, S. Revo, N. Gascoin, Structural and thermal characterization of multiwall carbon nanotubes (MWCNTs)/aluminum (Al) nanocomposites, Compos. B Eng. 151 (2018) 232–236, https://doi.org/10.1016/j.compositesb.2018.06.019.
[16] M. Yang, L. Weng, H. Zhu, F. Zhang, T. Fan, D. Zhang, Leaf-like carbon nanotube-graphene nanoribbon hybrid reinforcements for enhanced load transfer in copper matrix composites, Scripta Mater. 138 (2017) 17–21, https://doi.org/10.1016/j.scriptamat.2017.05.024.
[17] H. Wang, Y. Wang, X. Cao, M. Feng, G. Lan, Vibrational properties of graphene and graphene layers, J. Raman Spectrosc. 40 (2009) 1791–1796, https://doi.org/10.1002/jrs.2321.
[18] G. Wu, Z. Yu, L. Jiang, C. Zhou, G. Deng, X. Deng, Y. Xiao, A novel method for preparing graphene nanosheets/Al composites by accumulative extrusion-bonding process, Carbon 152 (2019) 932–945, https://doi.org/10.1016/j.carbon.2019.06.077.
[19] D.G. Papageorgiou, I.A. Kinloch, R.J. Young, Mechanical properties of graphene and graphene-based nanocomposites, Prog. Mater. Sci. 90 (2017) 75–127, https://doi.org/10.1016/j.pmatsci.2017.07.004.
[20] M. Komarasamy, T. Wang, K. Liu, L. Reza-Nieto, R.S. Mishra, Hierarchical multi-phase microstructural architecture for exceptional strength-ductility combination in a complex concentrated alloy via high-temperature severe plastic deformation, Scripta Mater. 162 (2019) 38–43, https://doi.org/10.1016/j.scriptamat.2018.10.033.
[21] Z.Y. Liu, B.L. Xiao, W.G. Wang, Z.Y. Ma, Singly dispersed carbon nanotube/aluminum composites fabricated by powder metallurgy combined with friction stir processing, Carbon 50 (2012) 1843–1852, https://doi.org/10.1016/j.carbon.2011.12.034.
[22] K. Chu, J. Wang, Y. Liu, Z. Geng, Graphene defect engineering for optimizing the interface and mechanical properties of graphene/copper composites, Carbon 140 (2018) 112–123, https://doi.org/10.1016/j.carbon.2018.08.004.
[23] Y. Huang, Y. Xie, X. Meng, J. Li, Atypical grain coarsening of friction stir welded AA6082-T6: characterization and modeling, Mater. Sci. Eng. A. (2019) 211–217, https://doi.org/10.1016/j.msea.2018.10.109, 740–741.
[24] C. Huang, S. Hu, K. Chen, Influence of rolling temperature on the interfaces and mechanical performance of graphene-reinforced aluminum-matrix composites, Int. J. Miner. Metall. Mater. 26 (2019) 752–759, https://doi.org/10.1007/s12613-019-1780-2.